JOURNAL OF MATERIALS SCIENCE 20 (1985) 391–398

Explosive shock loading of alpha-Si_3N_4 powder

J. J. PETROVIC, B. W. OLINGER, R. B. ROOF
Los Alamos National Laboratory, Los Alamos, New Mexico 87545, USA

Alpha-Si_3N_4 powders were explosively shock loaded at levels of 260 and 570 kbar pressure. Specimens exhibited densification without additives into the 93 to 98% dense range as a result of shock-induced consolidation. X-ray line broadening investigations indicated that significant residual, internal strain levels of the order of 0.4% were developed in the densified material. Hardness and indentation fracture toughness values for shock-densified regions were nearly equivalent to those for ultra-high-pressure hot-pressed Si_3N_4 without densification aids.

1. Introduction

Many ceramic materials of technological interest are difficult to consolidate, requiring in most instances high fabrication temperatures as well as the use of densification aids. Shock loading of ceramic powders is emerging [1]* as a technique for direct consolidation [2–9] as well as preconditioning of powders prior to consolidation by conventional methods [10–31].

The objective of the present investigation was to obtain an initial characterization of the response of alpha-Si_3N_4 powder subjected to the explosive shock loading environment. In this regard, a recently developed experimental approach allowed the convenient observation of effects of shock pressure, to pressures as high as 1000 kbar (100 GPa) with the routine recovery of shocked specimens. Thus, an initial examination of influences of shock pressure on the alpha-Si_3N_4 powder behaviour was made.

2. Experimental details

2.1. Material

A commercial alpha-Si_3N_4 powder† was employed for the investigation. The powder exhibited an average particle size of 0.3 μm, with a BET surface area of 23 $m^2 g^{-1}$. Phase analysis indicated 94% alpha-Si_3N_4, 3% beta-Si_3N_4, 3% SiO_2, and less than 0.1% free silicon. A scanning electron micrograph (SEM) of the as-received powder is shown in Fig. 1. The powder was observed to be a mixture of spherical particles as well as platelets. A spectrochemical analysis of impurities in the powder is given in Table I. Prior to explosive shock loading, the powder was cold-pressed into 3.18 mm diameter by 6.35 mm length pellets. No additives of any kind were incorporated in the Si_3N_4 pellets. The cold-pressed pellet density was 57% of the theoretical density of Si_3N_4.

2.2. Explosive shock loading

Fig. 2 shows the explosive shock loading assembly. The experimental configuration consisted of an array of concentric steel tubes, with the innermost tube made of copper to facilitate specimen removal by acid leaching away of the copper after test. The central copper tube was loaded with four Si_3N_4 pellets, each spaced 6.35 mm apart by copper spacers. This test assembly was surrounded by explosive (Composition C, a mixture of 91% cyclotrimethylene trinitramine (RDX), 2.1% polyisobutylene, 5.3% disebacate, and 1.6% motor oil, with a density of 1.59 g cm^{-3} and a detonation velocity of 8.04 mm μsec^{-1}) and then by a steel recovery ring. The explosive detonation initiates around the outer edge of the top of the specimen recovery cylinder, with the detonation wave moving down along the outer edge of the cylinder

*A bibliography of extensive studies in the Soviet Union is given by Graham *et al.*
†H. C. Starck LC-12.

0022–2461/85 $03.00 + .12

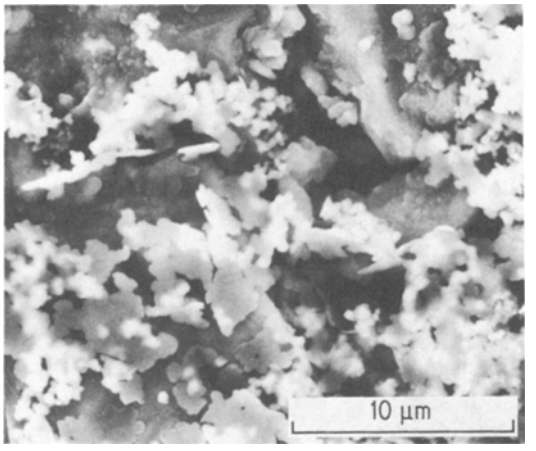

Figure 1 Scanning electron micrograph of as-received alpha-Si_3N_4 powder.

TABLE I Spectrochemical analysis of alpha-Si_3N_4 powder

Element	Weight ppm	Element	Weight ppm
Li	< 30	B	50
Mg	50	Ti	10
K	< 300	Fe	100
Cr	10	Zn	< 30
Ni	20	Y	< 10
Ge	< 30	Ag	< 1
Nb	< 30	Sb	< 100
In	< 30	Pb	< 30
Ta	< 0.1%	Na	< 100
Be	< 1	P	< 300
Al	200	V	< 10
Ca	50	Co	< 10
Mn	10	Ga	< 30
Cu	3	Zr	< 30
Sr	< 3	Cd	< 10
Mo	< 10	Ba	< 3
Sn	< 30	Bi	< 10
W	< 300		

and out into the explosive. The sweeping shock wave generated by the explosive coalescence along the axis of the cylinder creates a Mach disc. The terminal shock velocity achieved is the detonation velocity of the explosive, which determines the maximum pressure that can be achieved.

With this experimental arrangement, the specimens in the central tube experience increasing shock pressures with increasing distance down the tube length. At the top, the pressure is approximately 100 kbar, increasing to 1000 kbar at a position two-thirds of the way down the tube, then decreasing with further axial travel due to consumption of the explosive. The Si_3N_4 specimens were positioned so as to experience shock pressures of approximately 200, 500, 1000 and

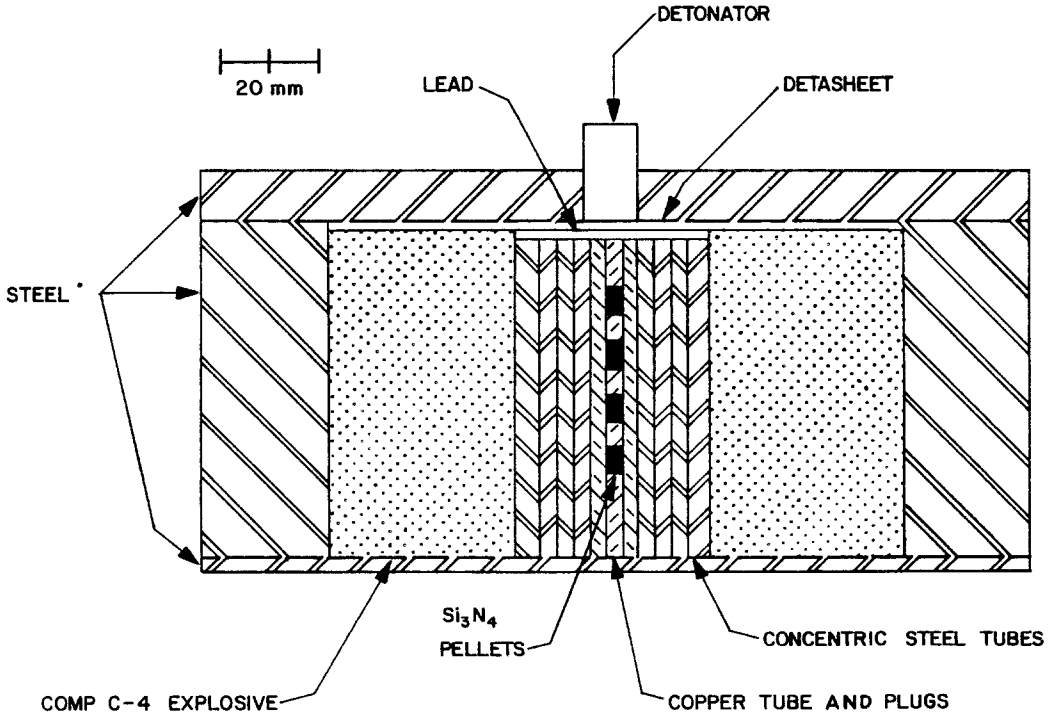

Figure 2 Explosive shock-loading assembly.

800 kbar. Shock pressures experienced by the Si_3N_4 specimens were determined using hydrocode computer calculations. These calculations employed a two-dimensional Eulerian code with abilities to incorporate multi-materials, inclusion of strengths and equations-of-state, and programmed burn for high-explosives.

2.3. X-ray line broadening

A material that has a large crystallite size (greater than 200 nm) and no non-uniform microcrystalline lattice strains will, in general, yield sharp X-ray diffraction lines. However, line broadening occurs when some physical operation changes the crystallite size from large to small and/or introduces large non-uniform microcrystalline lattice strains.

X-ray line broadening was measured by comparing shock-loaded X-ray peak widths with those of an unbroadened alpha-Si_3N_4 standard according to the formula:

$$\beta^2 = B^2 - b^2 \tag{1}$$

where B is the full peak width at half maximum intensity in radians for the shock-loaded material, and b the full peak width at half maximum intensity for the reference material.

X-ray line broadening from small particle effects is given by the following equation [32]:

$$\beta_p = \frac{\lambda}{d \cos\theta} \tag{2}$$

where λ is the X-ray wavelength, θ the Bragg diffraction angle, and d the crystallite size. Similarly, broadening due to lattice strains is given by [32]:

$$\beta_\epsilon = 4\epsilon \tan\theta \tag{3}$$

where ϵ is the lattice strain. A space averaged estimate of the crystallite size d and the lattice strain was obtained from X-ray data using the following equation [32]:

$$\beta^{*2} = (1/d)^2 + 16\epsilon^2 \sin^2\theta/\lambda^2 \tag{4}$$

where $\beta^* = (\beta)(\cos\theta/\lambda)$. Thus, using the linear form of Equation 4 for a number of alpha-Si_3N_4 X-ray peaks, the slope of the straight line was proportional to lattice strain, while the intercept was a measure of the crystallite size.

3. Results

After shock loading, only the first two pellets were successfully recovered since the pellets located at the 1000 and 800 kbar positions were essentially gone after the explosive event. The computer hydrocode was employed to determine shock pressure against time for the two recovered pellets, with results shown in Fig. 3. The pellet in position 1 experienced a peak pressure of 260 kbar while the pellet in position 2 saw a pressure of 570 kbar. Although these pressures were quite high, their duration was very short, less than 1 μsec.

Macro-photos of the two Si_3N_4 pellets after the shock exposure are shown in Fig. 4. Rather than retaining a powder morphology, the Si_3N_4 densified to 93% bulk density (as measured by an immersion technique) at 260 kbar shock pressure, with a more unusual response and lower bulk density at 570 kbar pressure. In order to clarify the higher pressure response, a second experiment was performed under nominally identical conditions. For this case, the 260 kbar specimen exhibited a 98.3% theoretical bulk density, while the 570 kbar specimen showed a 98.5% theoretical density and was similar in macroscopic appearance to the 260 kbar specimen shown in Fig. 4. This nonrepreducibility of the 570 kbar response suggests that this pressure range must be close to a transition regime for the Si_3N_4 which could be influenced by minor shock condition differences between the two experimental runs.

X-ray line broadening results are shown in Fig. 5, along with data obtained for Si_3N_4 powder shock loaded in gas gun experiments at approximately 8 and 24 kbar. No X-ray effects were observed at 8 kbar, with the crystallite size close to the particle size of the starting powder. However, at 24 kbar a decrease in the crystallite size and development of a small level of residual strain occurred, indicating the initial formation of atomic level defects in the powder. At 260 and 570 kbar pressure levels, a residual strain of nearly 0.4% was produced, while the crystallite size was reduced below 100 nm, indicating significant defect generation in the material. These results show that for alpha-Si_3N_4, marked shock loading effects occur in the 25 to 250 kbar shock pressure range.

A polished cross-section of the 260 kbar shock loaded Si_3N_4 specimen is shown in Fig. 6. As may be seen, the material is badly cracked, but the areas between the cracks are nearly fully densified. X-ray diffraction analysis indicated that there had been no change in the phase composition of the

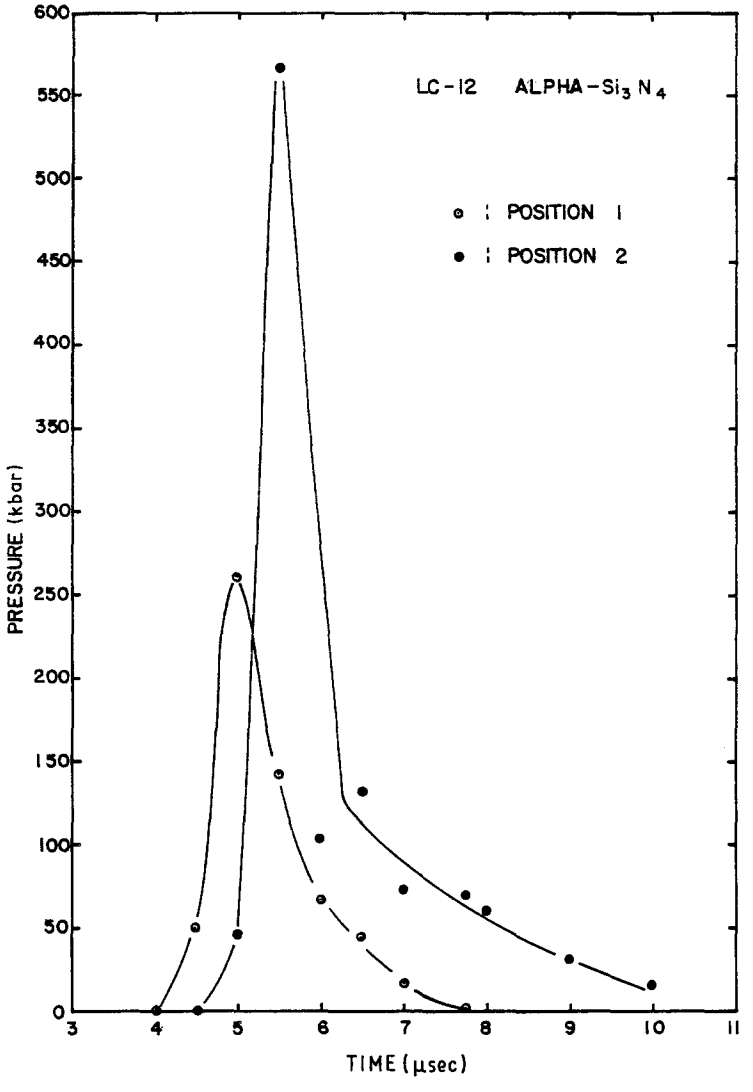

Figure 3 A plot of shock pressure against time for recovered alpha-Si_3N_4 pellets.

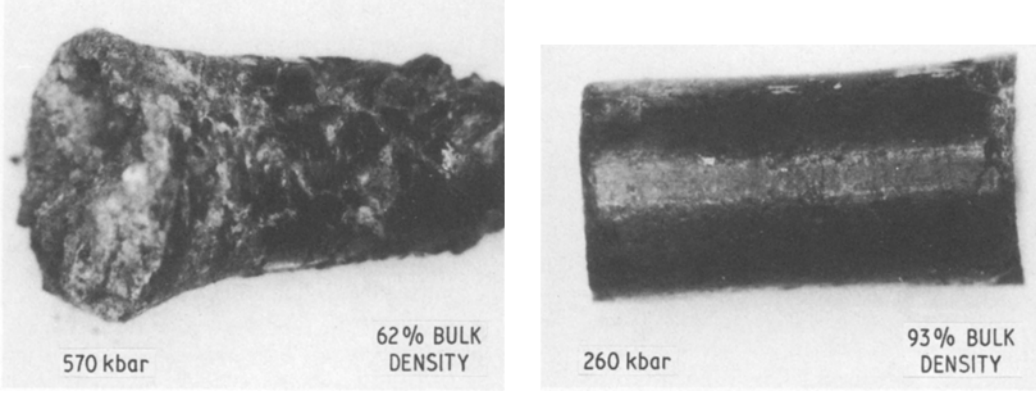

Figure 4 Macro-photos of Si_3N_4 pellets after shock loading.

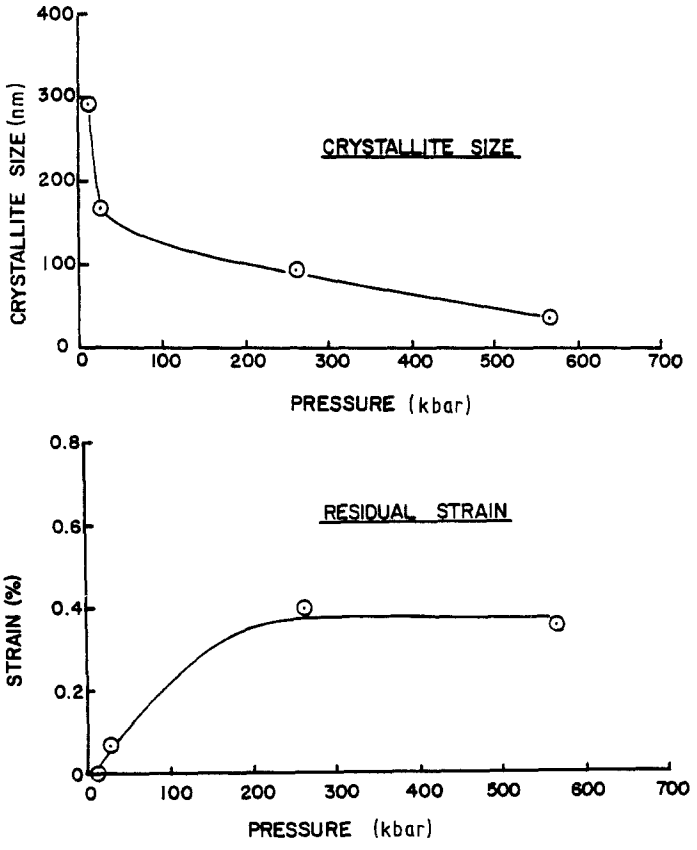

Figure 5 Shock-loaded Si_3N_4 X-ray line broadening results.

Si_3N_4 as a result of the shock consolidation. The densified material was still 94% alpha-Si_3N_4.

Vickers microhardness indentations (2000 g) were placed on the polished specimen in Fig. 6 to determine the hardness and indentation fracture toughness [33] of the densified Si_3N_4. One of these indentations is shown in Fig. 7. These indentations were in character virtually identical to those one might observe in a fully densified, hot-pressed Si_3N_4 material, indicating that the Si_3N_4 powder particles had been very strongly bonded together by the explosive densification process. As may be noted in Fig. 6, a hardness gradient exists in the Si_3N_4 specimen even though all regions are fully consolidated. This may reflect a gradient in shock-produced defect density within

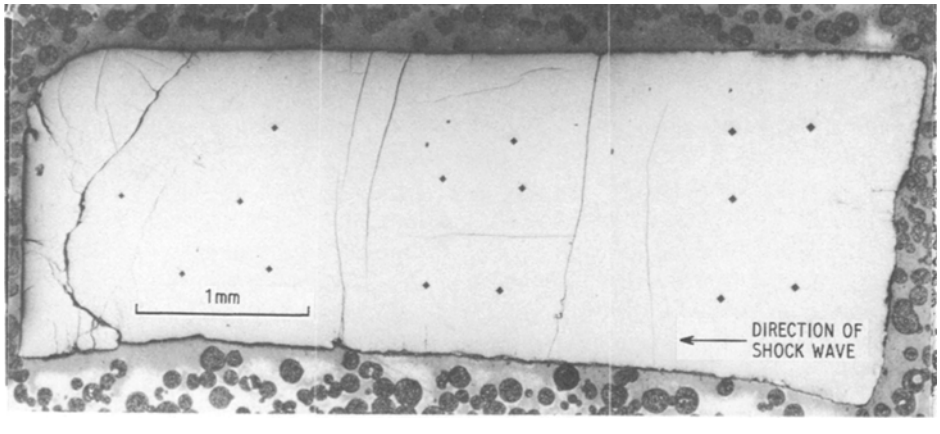

Figure 6 Polished cross-section of 260 kbar shock-loaded Si_3N_4 specimen. Vickers microhardness indentations appear as square-shaped dark features.

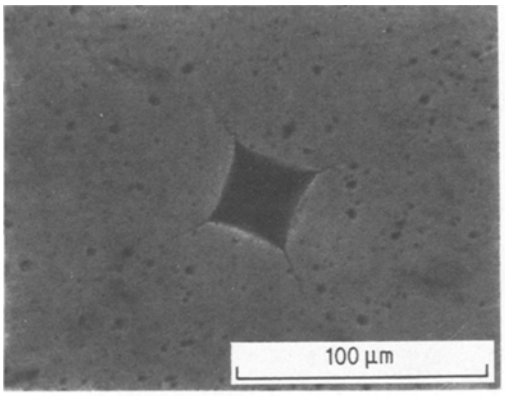

Figure 7 2000 g Vickers microhardness indentation in shock-consolidated alpha Si_3N_4.

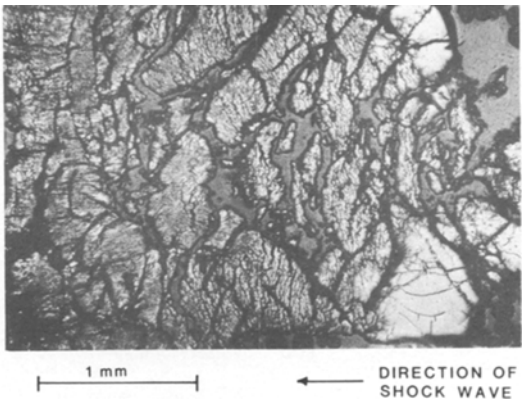

Figure 8 Polished cross-section of 570 kbar shock-loaded Si_3N_4 specimen.

the specimen. At the low gradient end, a Vickers hardness of 11.54 GPa was observed, while at the opposite end of the gradient a hardness of 17.87 GPa was measured. Indentation fracture toughness values obtained were 3.12 MPa $m^{1/2}$ in the low hardness region and 3.94 MPa $m^{1/2}$ in the high hardness region.

A polished cross-section of the 570 kbar specimen which exhibited the anomalous behaviour seen in Fig. 4 is shown in Fig. 8. Basically, the microstructure consists of a high density of very fine cracks. In order to determine if decomposition of the Si_3N_4 due to shock heating effects might be responsible for this morphology, X-ray analysis for the presence of free silicon was performed. No crystalline free silicon was detected, but this does not rule out the occurrence of decomposition, since such free silicon might have been amorphous. The phase composition of the 570 kbar material was, however, distinctly altered from 94% alpha-3% beta in the starting powder to 100% beta-Si_3N_4 for the material in Fig. 8. The second 570 kbar specimen which did not exhibit the unusual morphology showed a less drastic phase composition change to approximately 80% alpha-20% beta Si_3N_4.

Spectrochemical analysis of the shock-loaded Si_3N_4 powder indicated that it had elevated levels of copper (1700 wppm), iron (3000 wppm), tin (800 wppm), and lead (1200 wppm) after the shock loading treatment. In order to further analyse this impurity pick-up, the polished specimen in Fig. 6 was examined by electron microprobe, with the interior of the specimen traversed in 5 μm analysis steps. Small, isolated regions, 5 μm or less in extent, were observed with elevated concentrations of these impurities, indicating that the impurities were associated with isolated particles in the densified Si_3N_4 matrix. Thus, the impurities were not uniformly distributed throughout the Si_3N_4 consolidated body. The most likely source of the copper, tin, and iron is the shock-loading fixturing shown in Fig. 2. The source of the lead was probably the lead barrier between the detonator and the concentric steel tubes.

4. Discussion

Densification of alpha-Si_3N_4 without densification additives was observed under shock-loading conditions in the present investigation. In general, Si_3N_4 is a very difficult material to densify by present conventional consolidation methods and so densification aids have been relied on to synthesize bulk shapes [34]. Japanese investigators have been successful in achieving densification without additives [35], but only by resorting to ultra-high-pressure hot-pressing conditions of 1600° C and 30 kbar. Recently, Sawaoka [20] has also reported densification of alpha-Si_3N_4 powder to 97% theoretical density under 300 kbar shock-loading conditions, in agreement with our present results.

The X-ray line broadening results in Fig. 5 indicate that high levels of atomic defects are still present in the shock-consolidated Si_3N_4. The internal, residual strain level of 0.4% observed is very similar to levels reported for other shock-treated ceramic powders [24, 29, 36, 37]. For the explosive shock loading of a mixed alpha/amorphous Si_3N_4 powder at 270 kbar, dislocation densities of 10^{11} cm^{-2} are reported [29] with point defect levels of 10^{18} cm^{-3} [31].

The indentation mechanical properties of shock-densified alpha-Si_3N_4 may be compared to similar measurements made for alpha-Si_3N_4 powder consolidated by ultra-high-pressure hot-pressing without additives [38, 39]. These workers obtained values of Vickers microhardness of 19.6 GPa and indentation fracture toughness of 3.85 MPa $m^{1/2}$. Both of these values compare favourably to the properties obtained presently in the high hardness region of the shock-consolidated Si_3N_4.

For a powder particle body, the shock-loading event produces highly intense particle-to-particle contacts resulting in very high local pressures and possibly very high temperatures in addition, but only for an extremely short period of time (<1 μsec). The local high pressure aspect is somewhat analogous to the quasi-static situation beneath a microhardness indenter, where very high compressive stresses can produce significant plastic deformation and consequent high dislocation densities in otherwise brittle ceramic materials. Concerning shock temperature contributions, local melting of even high-melting point ceramics is a possible occurrence. Recent theoretical work [40] indicates that particle surface melting plays the dominant role in the shock consolidation of metal powders. The above suggest that the shock-loading introduction of defects is mechanistically controlled by high pressure, high loading rate, high temperature plastic deformation processes, possibly in association with local melting phenomena [37].

The fundamental question raised by the present Si_3N_4 shock-loading results is what is the mechanism of densification of this material under the shock conditions. One potential mechanism is compaction and local melting of the Si_3N_4 powder particle surfaces, such as most often occurs with metal powders [40]. Although Si_3N_4 does not melt, but rather decomposes, at elevated temperatures and ambient pressure, this mechanism cannot be ruled out under the ultra-high shock pressures. Another possible mechanism is large-scale plastic deformation of the Si_3N_4 particles, possibly coupled with melting of residual SiO_2 layers on the particle surfaces. Further detailed investigations are required in order to elucidate the Si_3N_4 shock-densification mechanism.

5. Conclusions

Explosive shock loading significantly affects alpha-Si_3N_4 powder. Large residual, internal strain levels of 0.4% strain are developed at 260 kbar and higher shock pressures, indicating the generation of high densities of atomic level defects. At 260 kbar shock pressure, consolidation of powders to nearly full density without densification additives occurs. The mechanical properties of the shock-consolidated Si_3N_4 are nearly identical to those for static, ultra-high-pressure hot-pressed Si_3N_4 without densification aids.

Acknowledgements

This work was supported by the Department of Energy, Division of Materials Sciences, Office of Basic Energy Sciences Under Contract No W-7405-ENG-36. We thank M. L. Lovato for assistance in specimen evaluation and M. Gibbs for experimental X-ray diffraction studies.

References

1. R. A. GRAHAM, B. MOROSIN and B. DODSON, "The Chemistry of Shock Compression: A Bibliography" (Sandia National Laboratories Report Sand 83-1887, October 1983).
2. R. J. CARLSON, S. W. POREMBKA and C. C. SIMONS, *Ceram. Bull.* **44** (1965) 266.
3. R. A. PRUEMMER and G. ZIEGLER, *Powder Met. Int.* 9 (1977) 11.
4. M. MITOMO and N. SETAKA, *J. Mater. Sci.* **16** (1981) 851.
5. C. L. HOENIG and C. S. YUST, *Ceram. Bull.* **60** (1981) 1175.
6. J. H. ADAIR, R. R. WILLS and V. D. LINSE, Proceedings, Emergent Process Methods for High Technology Ceramics, North Carolina State University, November (1982) p. 21.
7. V. D. LINSE and J. H. ADAIR, Conference Digest, American Physical Society Topical Conference on Shock Waves in Condensed Matter, Santa Fe, New Mexico, July (1983) p. 14.
8. J. J. PETROVIC, B. W. OLINGER and R. B. ROOF, Proceedings, American Physical Society Topical Conference on Shock Waves in Condensed Matter, Santa Fe, New Mexico, July (1983) p. 463.
9. S. SOGA, K. KONDO, A. SAWAOKA and M. ARAKI, *ibid.* (1983) p. 375.
10. M. J. KLEIN, F. A. ROUGH and C. C. SIMONS, *J. Amer. Ceram. Soc.* **46** (1964) 356.
11. O. R. BERGMANN and J. BARRINGTON, *ibid.* **49** (1966) 502.
12. M. J. KLEIN and P. S. RUDMAN, *Phil. Mag.* **14** (1966) 1199.
13. R. W. HECKEL and J. L. YOUNGBLOOD, *J. Amer. Ceram. Soc.* **51** (1968) 398.
14. H. SUZUKI, H. YOSHIDA and Y. KIMURA, *J. Ceram. Assoc. Japan.* 77 (1969) 36.
15. K. KAWADA and A. ONODERA, *Ceram. Bull.* 59 (1980) 1151.

16. A. SAWAOKA, S. SOGA and K. KONDO, *J. Mater. Sci. Lett.* **1** (1982) 347.
17. D. L. HANKEY, R. A. GRAHAM, W. F. HAMMETTER and B. MOROSIN, *ibid.* **1** (1982) 445.
18. R. A. GRAHAM, B. MOROSIN, E. VENTURINI, E. K. BEAUCHAMP and W. F. HAMMETTER, Proceedings, Emergent Process Methods for High Technology Ceramics, North Carolina State University, November (1982) p. 22.
19. E. K. BEAUCHAMP, R. E. LOEHMAN, R. A. GRAHAM and B. MOROSIN, *ibid.* (1982) p. 22.
20. A. SAWAOKA, *ibid.* (1982) p. 23.
21. K. Y. KIM, A. D. BATCHELOR and H. PALMOUR III, *ibid.* (1982) p. 13.
22. K. Y. KIM, H. PALMOUR III, A. D. BATCHELOR, H. KANDA, M. ASKAISHI and O. FUKUNAGA, Proceedings, American Physical Society Topical Conference on Shock Waves in Condensed Matter, Santa Fe, New Mexico, July (1983) p. 455.
23. H. PALMOUR III, K. Y. KIM, A. D. BATCHELOR, T. M. HARE, G. T. GOUDEY, K. L. MORE, V. D. LINSE and J. A. ADAIR, *ibid.* (1983) p. 459.
24. B. MOROSIN, R. A. GRAHAM and J. R. HELLMANN, *ibid.* (1983) 383.
25. J. R. HELLMANN, K. KURODA, A. H. HEUER and R. A. GRAHAM, *ibid.* (1983) p. 387.
26. W. F. HAMMETTER, J. R. HELLMANN, R. A. GRAHAM and B. MOROSIN, *ibid.* (1983) p. 391.
27. E. K. BEAUCHAMP, R. A. GRAHAM and B. MOROSIN, Conference Digest, American Physical Society Topical Conference on Shock Waves in Condensed Matter, Santa Fe, New Mexico, July (1983) p. 40.
28. Y. K. LEE, F. L. WILLIAMS, R. A. GRAHAM and B. MOROSIN, Proceedings, American Physical Society Topical Conference on Shock Waves in Condensed Matter, Santa Fe, New Mexico, July (1983) p. 399.
29. R. E. LOEHMAN, E. K. BEAUCHAMP and R. A. GRAHAM, Conference Digest, American Physical Society Topical Conference on Shock Waves in Condensed Matter, Santa Fe, New Mexico, July (1983) p. 41.
30. M. J. CARR and E. K. BEAUCHAMP, Proceedings, American Physical Society Topical Conference on Shock Waves in Condensed Matter, Santa Fe, New Mexico, July (1983) p. 403.
31. E. L. VENTURINI, R. A. GRAHAM and B. MOROSIN, Conference Digest, American Physical Society Topical Conference on Shock Waves in Condensed Matter, Santa Fe, New Mexico, July (1983) p. 41.
32. C. N. J. WAGNER, "Local Atomic Arrangements Studied by X-ray Diffraction" (Gordon and Breach, New York, 1966) p. 219.
33. G. R. ANSTIS, P. CHANTIKUL, B. R. LAWN and D. B. MARSHALL, *J. Amer. Ceram. Soc.* **64** (1981) 533.
34. F. F. LANGE, *Ceram. Bull.* **62** (1983) 1369.
35. T. YAMADA, M. SHIMADA and M. KOIZUMI, *ibid.* **60** (1981) 1281.
36. B. MOROSIN and R. A. GRAHAM, Proceedings, American Physical Society Topical Conference on Shock Waves in Condensed Matter, Santa Fe, New Mexico, July (1983) p. 355.
37. R. F. DAVIS, Y. HORIE, R. O. SCATTERGOOD and H. PALMOUR III, Proceedings, International Symposium on Structure-Property Relationships for MgO and Al_2O_3 Ceramics, Massachusetts Institute of Technology, Cambridge, Massachusetts, June (1983).
38. M. SHIMADA, M. KOIZUMI, A. TANAKA and T. YAMADA, *J. Amer. Ceram. Soc. Commun.* **65** (1982) C-48.
39. K. TSUKUMA, M. SHIMADA and M. KOIZUMI, *Ceram. Bull.* **60** (1981) 910.
40. R. B. SCHWARZ, P. KASIRAJ, T. VREELAND and T. J. AHRENS, *Acta Metall.* in press.

Received 15 February
and accepted 9 March 1984